Person Identification System Using Fusion of Matching Score of Iris

Yogeshwari Borse[1], Rajnish Choubey[1], Roopali Soni[1], Milind E. Rane[2]

**[1] Computer Science Engineering Department, RGP University ,
Bhopal, Madhyapradesh, India**

**[2] Electronics Engineering Department, Vishwakarma Institute of Technology,
University of Pune, Maharashtra, India**

Abstract

Human iris provides a unique structure suitable for non-invasive biometric assessment. In particular the irises are as distinct as fingerprints even for twins. In this paper a system for person identification is presented that uses a technique of localization, alignment, feature extraction, matching the features of irises and finally the decision regarding the degree of match based on hamming distance. A CASIA iris database of iris images has been used in the implementation of the iris recognition system. The results show that proposed method is quite effective.

Keywords: *Iris recognition, Iris Localization, decision level fusion.*

1. Introduction

Biometric verification has been receiving extensive attention over the past decade with increasing demands in automated personal identification. Biometrics deals with the uniqueness of an individual arising from their physiological or behavioral characteristics for the purpose of personal identification. Biometric recognition [1] systems verify a person's identity by analyzing his/her physical features or behavior (e.g. face [2], fingerprint, voice, signature, keystroke rhythms). Among many biometrics techniques, iris recognition is one of the most promising approaches due to its high reliability for personal identification [1–8]. Iris recognition is a method of biometric authentication that uses pattern recognition techniques based on high-resolution images of the irises of an individual's eyes. A major approach for iris recognition today is to generate feature vectors corresponding to individual iris images and to perform iris matching based on some distance metrics [3–6]. Most of the commercial iris recognition systems implement a famous algorithm using iris codes proposed by Daugman [3]. Iris recognition uses camera technology, with subtle infrared illumination reducing specular reflection from the convex cornea, to create images of the detail-rich, intricate structures of the iris. Converted into digital templates, these images provide mathematical representations of the iris that yield unambiguous positive identification of an individual. One of the difficult problems in feature-based iris recognition is that the matching performance is significantly influenced by many parameters in feature extraction process (eg., spatial position, orientation, center frequencies and size parameters for 2D Gabor filter kernel), which may vary depending on environmental factors of iris image acquisition. The human iris contains around 266 visible patterns, which forms the basis of several recognition algorithms [5]. Even on the same person, left and right irises are different. The iris is unique to an individual and is stable with age [6]. This is a key advantage of iris recognition as its stability, or template longevity as, barring trauma, a single enrollment can last a lifetime. Wildes [9] started the segmentation of the iris ring by the construction of a binary edge-map. Next, used the circular Hough transform to fit circles that delimit the iris ring. This is the most usually seen method in the iris segmentation literature and is proposed with minor variants by [10-13]. Proenca et al. proposed a method [14] that uses a clustering process to increase the robustness to noisy data. The method proposed by Du et al. [15] is based on the previous detection of the pupil. The image is then transformed into polar coordinates and the iris outer border localized as the largest horizontal edge resultant from Sobel filtering. Morphologic operators were applied by Mira et al. [16] to find both iris borders. They detected the inner border by sequentially using threshold, image opening and closing techniques. The outer border was similarly detected. Eric Sung et al. proposed complexity measure based on maximum Shannon entropy of wavelet packet reconstruction to quantify the iris information [17]. Jiali Cui et al. proposed [18] the iris recognition algorithm based on PCA (Principal Component Analysis) is first introduced and then, iris image synthesis method is presented. Lee et al. have introduced [19] the invariant binary feature which is defined as iris key. Kazuyuki et al.

developed [20] phase-based image matching algorithm. Fusion of more than one biometrics makes the system more robust and accurete[21-22]. The fusion of different biometrics can be done at various levels, namely, sensor level, feature level[23], matching score level[24] and decision level. Fusion of multiple biometrics ie. Multiple snapes of Iris makes possible to achieve highly robust identification in a unified fashion with a simple matching algorithm. In this paper a biometric system based on fusion of decision level for iris features is proposed for robust personal identification. It consist of a technique of localization, alignment, feature extraction, matching the features of irises and finally the fusion is made for decision regarding the degree of match.

This paper has been organized in the following way. The iris recognition system is divided into three parts: image acquisition, iris localization and pattern matching. Image acquisition, iris localization are described in Section 2. In Section 3 and 4 , the algorithm of this system is explained. Section 5 defines the matching by calculating the modified Hamming distance. Section 6 gives the fusion of decision for identification. Finally the results obtained and concluding remarks are mentioned.

2. Proposed Iris Recognition System

Block diagram of the proposed iris recognition system is as shown in Figure 1 that contains the typical stages of iris recognition system. A general block diagram of how Biometric system works is shown in Figure 1

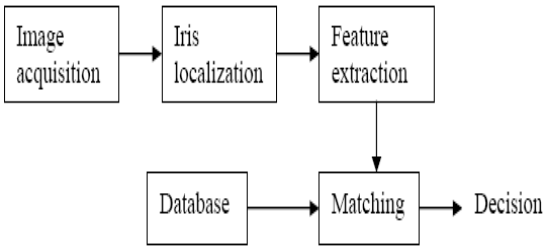

Fig 1. Proposed iris recognition system

The initial stage concerns about the segmentation of the iris. This consists in localize the iris inner (pupillary) and outer (scleric) boundaries, assuming either circular or elliptical shapes for each border. Additionally, it is used to detect regions of the iris texture occluded by any other type of data, as eyelids, eyelashes, glasses or hair. Extracted iris image are normalized and using Log Gabor transform features are extracted. These extracted features are stored in the database during enrollment. While matching features of the query image are correlated with the feature vectors of templates in the database and decision is formulated.

2.1 Image acquisition

The system captures eye images with the iris diameter typically between 100 and 200 pixels from a distance of 15–46 cm using a 330-mm lens.

2.2 Iris localization:

Image acquisition of the iris cannot be expected to yield an image containing only the iris. It will also contain data derived from the surrounding eye region. Therefore, prior to iris pattern matching, it is important to localize that portion of the image derived from inside the limbs (the border between the sclera and the iris) and outside the pupil. If the eyelids are occluding part of the iris, then only that portion of the image without the eyelids should be included.

For the localization of iris first any random circular contour is formed which contains iris + pupil region to eliminate the remaining portion of the eye. A circular pseudo image is formed of desired diameter. The inside region of the circle is set at gray level ‘1’(white) and the outside region to ‘0’(black). The diameter selected is such that the circular contour will encircle the entire iris. This diameter selection is crucial as it should be common for all iris images. Thus when the product of the gray levels of the circular pseudo image and the original iris image are taken, the resultant image will have the circular contour enclosing the iris patterns and the outside of the circular contour will be at gray level ‘0’(black).

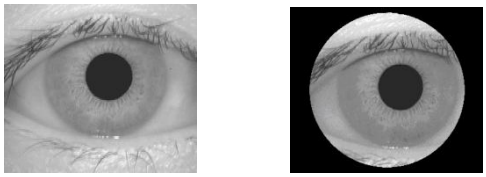

(a) (b)

Fig 2. (a)eye image (b) circular contour around iris

The resultant image is the localized iris image. This circular contour is moved such that it is concentric with the pupil. So before pattern-matching, alignment is carried out. The iris and pupilary boundary of the iris are concentric about the pupilary center. So our aim is to determine the pupilary center. Firstly, we use point image processing techniques such as thresholding and gray-level slicing (without the background) on the resultant localized image to eliminate every other feature except the pupil of the eye. The pupil of the eye is set at gray level ‘0’ and rest of the region is at ‘255’(white) .Next step involves determining the center of the pupil.

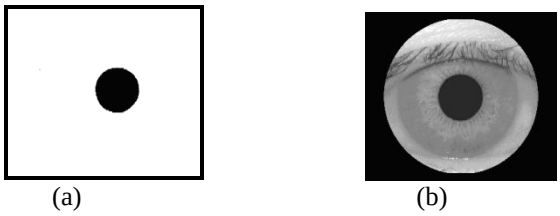

Fig 3. (a) Binary Pupil (b) Alignment of Iris

This is done by finding the row and column having the maximum number of pixels of gray level '0' (black), which corresponds to the center of the pupil. Knowing the center of the pupil, we now shift the center of the circular contour to the center of the pupil. The resultant image will have the pupil and the iris regions concentric with the circular contour and the localized iris image to the center of frame is performed as shown in Figure 3. Pupil diameter is known to us and to find iris diameter get binary image of semi circular iris using image point processing operators, mainly gray level slicing with and without the background and a digital negative, we obtain only the iris at gray level '0'(black) and the remaining portion of the image is at gray level '255'(white) . The shape of the iris in this case can be considered to be semi-circular.

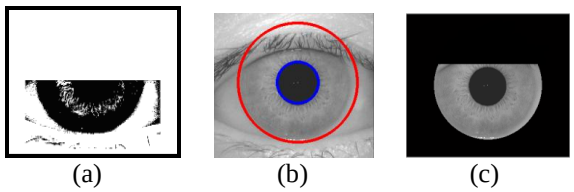

Fig 4. (a) Binary Semi-Iris Image (b) Localized iris (c) Image removing eyelids

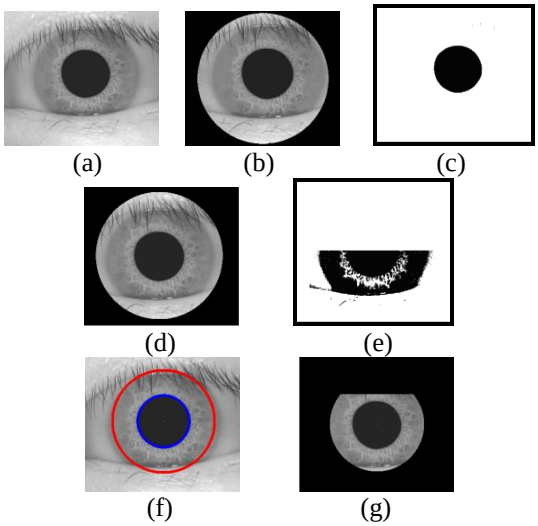

Fig 5. (a)eye image (b) circular contour around iris (c) Binary Pupil Image (d) Alignment of Iris (e) Binary Semi-Iris Image (f) Localized iris (g) Image removing eyelids

Now scanning row-wise, a counter determines the number of pixels having gray level '0' (white) in each row and the maximum count can be considered as the diameter of the iris along the row. Now scanning column-wise, a counter determines the number of pixels having gray level '0' (white) in each column and the maximum count can be considered as the radius of the iris. Doubling gives the diameter of the iris along the column. Taking the average of the two, we get the average iris diameter. Final Result of iris localization eye with iris and pupil are circled correctly.

Removing the portion of the iris occluded by the eyelids is carried out next. The eyelids are occluding part of the iris, so only that portion of the image below the upper eyelids and above the lower eyelids are included. This is achieved by changing the gray level above the upper eyelids and below the lower eyelids to '0'. Figure 5 shows entire steps performed on another eye image.

3. Feature extraction

Once the iris region is successfully segmented from an eye image, the next stage is to transform the iris region so that it has fixed dimensions in order to allow comparisons. The dimensional inconsistencies between eye images are mainly due to the stretching of the iris caused by pupil dilation from varying levels of illumination. Other sources of inconsistency include, varying imaging distance, rotation of the camera, head tilt, and rotation of the eye within the eye socket. The normalization process will produce iris regions, which have the same constant dimensions. The homogenous rubber sheet model devised by Daugman [8] remaps each point within the iris region to a pair of polar coordinates (r, θ) where r is on the interval [0, 1] and θ is angle [0,2π].

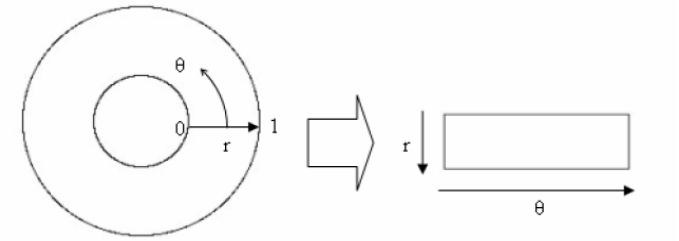

Fig 6. Daugman's Rubber Sheet Model.

The remapping of the iris region from (x, y) Cartesian coordinates to the normalized non-concentric polar representation is modeled as Eq. 1.

$$I(x(r,\theta), y(r,\theta)) = I(r,\theta) \quad (1)$$

with

$$x(r,\theta) = (1-r)xp(\theta) + rxi(\theta)$$
$$y(r,\theta) = (1-r)yp(\theta) + r\,yi(\theta)$$

Where $I(x,y)$ is the iris region image, (x,y) are the original Cartesian coordinates, (r,θ) are the corresponding normalized polar coordinates, and xp, yp and xi, yi are the coordinates of the pupil and iris boundaries along the θ direction. The rubber sheet model takes into account pupil dilation and size inconsistencies in order to produce a normalized representation with constant dimensions. In this way the iris region is modeled as a flexible rubber sheet anchored at the iris boundary with the pupil centre as the reference point.

Even though the homogenous rubber sheet model accounts for pupil dilation, imaging distance and non-concentric pupil displacement, it does not compensate for rotational inconsistencies. In Daugman system, rotation is accounted for during matching by shifting the iris templates in the θ direction until two iris templates are aligned.

For normalization of iris regions a technique based on Daugman's rubber sheet model was employed. The centre of the pupil was considered as the reference point, and radial vectors pass through the iris region, as shown in Figure 6. A number of data points are selected along each radial line and this is defined as the radial resolution. The number of radial lines going around the iris region is defined as the angular resolution. Since the pupil can be non-concentric to the iris, a remapping formula is needed to rescale points depending on the angle around the circle. This is given by Eq.2.

$$r' = \sqrt{\alpha\beta} \pm \sqrt{\alpha\beta^2 - \alpha - r_I^2} \qquad (2)$$

with

$$\alpha = O_x^2 + O_y^2$$

and

$$\beta = COS(\pi - \arctan(\frac{O_x}{O_y}) - \theta)$$

where displacement of the center of the pupil relative to the center of the iris is given by $O_{x,}, O_y$, and r' is the distance between the edge of the pupil and edge of the iris at an angle, θ around the region, and r' is the radius of the iris as shown in Figure 7. The remapping formula first gives the radius of the iris region 'doughnut' as a function of the angle θ.

A constant number of points are chosen along each radial line, so that a constant number of radial data points are taken, irrespective of how narrow or wide the radius is at a particular angle. From the 'doughnut' iris region, normalization produces a $2D$ array with horizontal dimensions of angular resolution and vertical dimensions of radial resolution. Another $2D$ array was created for marking reflections, eyelashes, and eyelids detected in the segmentation stage. In order to prevent non-iris region data from corrupting the normalized representation, data points which occur along the pupil border or the iris border are discarded.

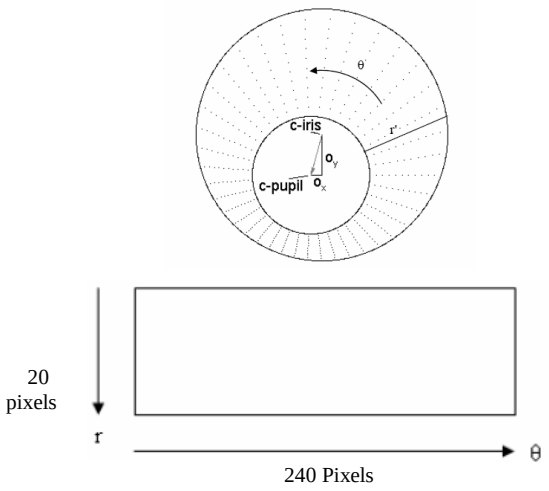

Fig 7. Normalization with radial resolution of 20 pixels, and angular resolution of 240 pixels.

The normalization process proved to be successful, a constant number of points are chosen along each radial line, here 20 pixel points are chosen as number of radial data points are taken, and 240 pixel points for angular data points are selected to create a $2D$ array, as shown in Figure 8.

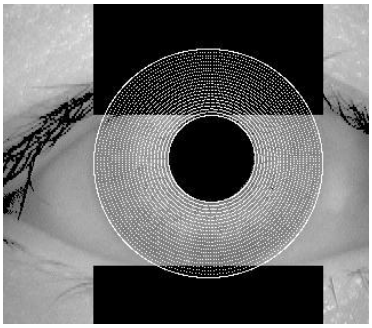

Fig 8. Radial and angular pixel from iris region

4. Feature Encoding

After iris region is segmented, to provide accurate recognition of individuals, the most discriminating information present in an iris pattern must be extracted to create a biometric template. Only the significant features of the iris must be encoded so that comparisons between templates can be made. Gabor filters are able to provide optimum conjoint representation of signal in space and spatial frequency.

Normalization produces a $2D$ array with horizontal dimensions of angular resolution and vertical dimensions of radial resolution as shown in Figure 9.

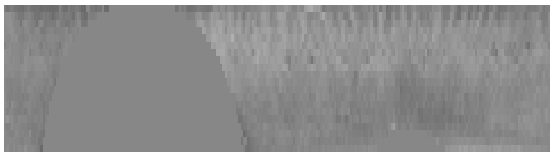

Fig 9. Normalized Iris (Polar array)

Another $2D$ array for marking reflections, eyelashes, and eyelids to prevent non-iris region data from corrupting the normalized representation, as shown in Figure 10 below.

Fig 10. Mask for normalized iris (Polar Mask)

A Gabor filter is constructed by modulating a sine/cosine wave with a Gaussian. This is able to provide the optimum conjoint localization in both space and frequency, since a sine wave is perfectly localized in frequency, but not localized in space. Modulation of the sine with a Gaussian provides localization in space, though with loss of localization in frequency. Decomposition of a signal is accomplished using a quadrature pair of Gabor filters, with a real part specified by a cosine modulated by a Gaussian, and an imaginary part specified by a sine modulated by a Gaussian. The real and imaginary filters are also known as the even symmetric and odd symmetric components respectively.

The centre frequency of the filter is specified by the frequency of the sine/cosine wave, and the bandwidth of the filter is specified by the width of the Gaussian.

Daugman makes uses of a $2D$ version of Gabor filters in order to encode iris pattern data. A $2D$ Gabor filter over the an image domain (x,y) is represented as Eq.3.

$$G(x,y)=e^{-\pi[(x-x_0)^2/\alpha^2+(y-y_0)^2/\beta^2]}e^{-2\pi i[u_0(x-x_0)+v_0(y-y_0)]} \quad (3)$$

where x_0, y_0 specify position in the image, (α,β) specify the effective width and length, and (uo, vo) specify modulation, which has spatial frequency $\omega=\sqrt{u_0^{\,2}+v_0^{\,2}}$. The odd symmetric and even symmetric $2D$ Gabor filters are shown in Figure 11.

Daugman demodulates the output of the Gabor filters in order to compress the data. This is done by quantizing the phase information into four levels, for each possible quadrant in the complex plane, phase information, rather than amplitude information provides the most significant information within an image. Taking only the phase will allow encoding of discriminating information in the iris, while discarding redundant information such as illumination, which is represented by the amplitude component.

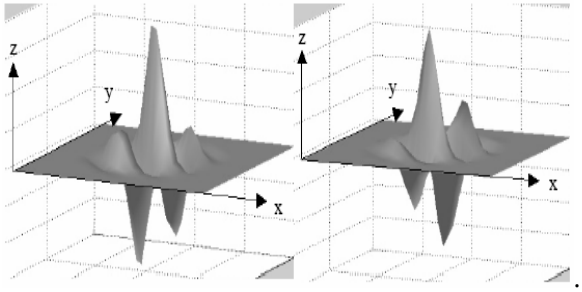

Figure 11 – A quadrature pair of 2D Gabor filters left- real component or even symmetric filter characterized by a cosine modulated by a Gaussian, right- imaginary component or odd symmetric filter characterized by a sine modulated by a Gaussian.

These four levels are represented using two bits of data, so each pixel in the normalized iris pattern corresponds to two bits of data in the iris template. A total bits are calculated for the template, and an equal number of masking bits are generated in order to mask out corrupted regions within the iris. This creates a compact template, which comparison of irises. The Daugman system makes use of polar coordinates for normalization, therefore in polar form the filters are given as Eq. 4

$$H(r,\theta)=e^{-i\omega(\theta-\theta_o)}e^{-(r-r_o)^2/\alpha^2}e^{-i(\theta-\theta_0)^2/\beta^2} \quad (4)$$

Where (α,β) are the same as in Eq. 3 and (r_0,θ_0) specify the centre frequency of the filter.

The demodulation and phase Quantization process can be represented as Eq. 5

$$h_{(\mathrm{Re,Im})}=\mathrm{sgn}_{(\mathrm{Re,Im})}\int_{\rho}\int_{\phi} I(\rho,\phi)e^{-i\omega(\theta_o-\phi)}e^{-(r_o-\rho)^2/\alpha^2}e^{-(\theta_o-\phi)^2/\beta^2}\rho\,d\rho\,d\phi \quad (5)$$

where $h_{(\mathrm{Re,Im})}$ can be regarded as a complex valued bit whose real and imaginary components are dependent on the sign of the $2D$ integral, and is the raw iris image in a dimensionless polar coordinate system.

A disadvantage of the Gabor filter is that the even symmetric filter will have a DC component whenever the bandwidth is larger than one octave .However, zero DC component can be obtained for any bandwidth by using a Gabor filter which is Gaussian on a logarithmic scale, this is known as the Log-Gabor filter. The frequency response of a Log-Gabor filter is given as in Eq. 6;

$$G(f) = \exp\left(\frac{-(\log(f / f_o))^2}{2(\log(\sigma / f_o^2))}\right) \quad (6)$$

Where f_o represents the centre frequency, and σ gives the bandwidth of the filter.

5. Matching

In comparing the bit patterns X and Y, the Hamming distance, HD, is defined as the sum of disagreeing bits (sum of the exclusive-OR between X and Y) over N, the total number of bits in the bit pattern as given in Eq. 7.

$$HD = \frac{1}{N}\sum_{j=1}^{N} X_j (XOR) Y_j \quad (7)$$

For matching, the Hamming distance was chosen as a metric for recognition, since bit-wise comparisons were necessary. The Hamming distance algorithm employed also incorporates noise masking, so that only significant bits are used in calculating the Hamming distance between two iris templates. Now when taking the Hamming distance, only those bits in the iris pattern that corresponds to '0' bits in noise masks of both iris patterns will be used in the calculation. The Hamming distance will be calculated using only the bits generated from the true iris region, and this modified Hamming distance formula is given as Eq. 8.

$$HD = \frac{1}{N - \sum_{K=1}^{N} Xn_k (OR) Yn_k} \sum_{j=1}^{N} X_j (XOR) Y_j (AND) Xn_j^{'} (AND) Yn_j^{'} \quad (8)$$

Where X_j and Y_j are the two bit-wise templates to compare, X_{nj} and Y_{nj} are the corresponding noise masks for X_j and Y_j, and N is the number of bits represented by each template.

In order to account for rotational inconsistencies, when the Hamming distance of two templates is calculated, one template is shifted left and right bit-wise and a number of Hamming distance values are calculated from successive shifts. This bit-wise shifting in the horizontal direction corresponds to rotation of the original iris region by an angle given by the angular resolution used. This method is suggested by Daugman, and corrects for misalignments in the normalized iris pattern caused by rotational differences during imaging. From the calculated Hamming distance values, only the lowest is taken, since this corresponds to the best match between two templates.

6. Fusion of Decision level

For the robust recognition two iris images are used for fusion at decision level. With these two images, find the two Hamming distance of test images with Query. Two hamming distances are given by D1 and D2. If D1 or D2 is less than Threshold the image is recognized. Otherwise it is rejected. This makes the algorithm robust to accept the person under query.

7. Result

The result obtained after experimentation are calculated. The percentage Accuracy Based on FAR (False Acceptance Ratio), FRR (False Reject Ratio) and RAR (Right Acceptance Ratio) of the implemented algorithm is given in Table 1 for single biometrics and Table 2 gives the result for Fusion of Iris at decision level as given below.

Table 1. Result interms of RAR, FRR, FAR for Single Iris image.

Threshold	RAR	FRR	FAR
0.3	68	32	0.0408
0.35	86.66	13.33	0.040
0.4	92.66	7.33	0.0816
0.435	94.66	5.33	2.64
0.45	97.33	2.66	11.93

Table 2. Result interms of RAR, FRR, FAR for Multiple Iris image.

Threshold	RAR	FRR	FAR
0.3	89.33	10.66	0
0.35	96	4	0
0.4	98.66	1.33	0.04
0.435	99.33	0.66	2.87
0.45	100	0	15.41

8. Conclusions

The developed system of Biometrics using fusion at decision level for person identification is tested and the results are all described earlier, shows a good separation of intra-class and inter-class for different persons. If selected threshold is changed according to determined Hamming Distances such that if we select the maximum Hamming distance of that particular Person, and considering same as threshold for decision it can improve decision making accuracy. As mentioned in result the recognition rate gets improved due to the fusion of multiple iris images. The results obtained are more robust in multimodal system as compared to single biometrics system.

References

[1] Jain A. K., Ross A, Prabhakar S. "An introduction to biometric recognition," IEEE transactions on circuits and systems for video technology—special issue on image and video-based biometrics, vol. 14(1); 2004.

[2] Satyajit Kautkar, Rahulkumar Koche, Tushar Keskar, Aniket Pande, Milind Rane, Gary A. Atkinson, "Face Recognition Based on Ridgelet Transforms," Procedia Computer Science 2 (ICEBT 2010), pp. 35–43.

[3] Daugman J G, "Recognizing people by their iris patterns," Information Security Technical Report, Volume 3, Issue 1, 1998, Pages 33-39.

[4] Daugman J G, "Recognizing people by their iris patterns," Information Security Technical Report, Volume 4, Supplement 1, 1999, Page 29.

[5] Daugman J G, "The importance of being random: statistical principles of iris recognition," Pattern Recognition, Volume 36, Issue 2, February 2003, Pages 279-291.

[6] Daugman J G, "How Iris Recognition Works," Handbook of Image and Video Processing (Second Edition), 2005, Pages 1251-1262.

[7] Kawaguchi, T, Rizon, M, "Iris detection using intensity and edge information," Pattern Recognition, Volume 36, Issue 2,, February 2003, Pages 549-562.

[8] Bowyer, K W, Hollingsworth, K P, Flynn, P J, "Image Understanding for Iris Biometrics: A survey," CVIU, May 2008, Pages 281-307.

[9] Wildes R.P., "Iris recognition: an emerging biometric technology," Proceedings of the IEEE, vol. 85(9);1997. p. 1348–63.

[10] L. Ma, T. Tan, Y. Wang, and D. Zhang., "Personal Identification Based on Iris Texture Analysis," IEEE Transactions on Pattern Analysis and Machine Intelligence, 25(12), pp.1519-1533, December 2003.

[11] L. Ma, Y. Wang, and D. Zhang, "Efficient iris recognition by characterizing key local variations," IEEE Transactions on Image Processing, vol. 13, no. 6, pp. 739–750, June

[12] J. Huang, Y. Wang, T. Tan, and J. Cui, "A new iris segmentation method for recognition," in Proceedings of the 17th International Conference on Pattern Recognition (ICPR04), vol. 3, 2004, pp. 23–26.

[13] L. Ma, Y. Wang, and T. Tan, "Iris recognition using circular symmetric filters," in Proceedings of the 25th International Conference on Pattern Recognition (ICPR02), vol. 2, 2002, pp. 414–417.

[14] H. Proenca and L. A. Alexandre, "Iris segmentation methodology for non-cooperative iris recognition," IEE Proc. Vision, Image & Signal Processing, vol. 153, issue 2, pp. 199–205, 2006.

[15] Y. Du, R. Ives, D. Etter, T. Welch, and C. Chang, "A new approach to iris pattern recognition," in Proceedings of the SPIE European Symposium on Optics/Photonics in Defence and Security, vol. 5612, October 2004, pp. 104–116.

16] J. Mira and J. Mayer, "Image feature extraction for application of biometric identification of iris - a morphological approach," in Proceedings of the 16th Brazilian Symposium on Computer Graphics and Image Processing (SIBGRAPI 2003), Brazil, 2003, pp. 391–398.

[17] E. Sung, X. Chen, J. Zhu and J. Yang, "Towards non-cooperative iris recognition systems", Seventh international Conference on Control, Automation, Robotics And Vision (ICARCV'02), Dec. 2002, Singapore, pp. 990-995.

[18] J. Cui, Y. Wang, J. Huang, T. Tan and Z. Sun, "An Iris Image Synthesis Method Based on PCA and Super-resolution", IEEE CS Proceedings of the 17th International Conference on Pattern Recognition (ICPR'04).

[19] H. Gu Lee, S. Noh, K. Bae, K.-R. Park and J. Kim, "Invariant biometric code extraction", IEEE Intelligent Signal Processing and Communication Systems (ISPACS 2004), Proceedings IEEE ISPACS, 2004, pp. 181-184.

[20] K Miyazawa, K Ito, T Aoki, K Kobayashi, H. Nakajima, "An Efficient Iris Recognition Algorithm Using Phase-Based Image Matching", IEEE Image Processing Conference, 2005 (ICIP 2005), 11-14 Sept. 2005, Vol. 2, pp. II- 49-52.

[21] A. K. Jain and A. Ross, "Multibiometric systems", Communications of the ACM, 47 (1), pp. 34-40, 2004.

[22] A. Ross and A.K. Jain, "Information Fusion in Biometrics", Pattern Recognition Letters, 24, pp. 2115-2125, 2003.

[23] A. Rattani, D. R. Kisku, M. Bicego, Member and M. Tistarelli, "Feature Level Fusion of Face and Fingerprint Biometrics," IEEE Concerence,2007.

[24] M. Hanmandlu, Amioy Kumar, Vamsi Madasu, Prasad Yarlagadda, "Fusion of Hand Based Biometrics using Particle Swarm optimization", 5th International Conference on Information Technology: New Generations, pp.783-788, 2008.

[25] Chinese Academy of Sciences. Specification of CASIA Iris Image Database (ver1.0) March 2007 .

Yogeshwari Borse received B.E.Computer Engg.-- North Maharashtra University, India. She is currently pursuing M.Tech from computer Science & Engg. Department in Thakral College of Technology, Bhopal, RGP University , India.

Rajnish Choubey received M. Tech. (CTA) Hon's. From UTD, RGP University, Bhopal in 2008 . He is currently working with computer Science & Engg. Department in Thakral College of Technology, Bhopal.

Roopali Soni received M.Tech degree from SOIT, RGP university in Computer Technology and Application. She is currently Head of computer Science & Engg. Department in Thakral College of Technology, Bhopal. Her research interests include soft computing Data Mining and warehousing and Object Oriented Concepts. Ms.Soni is a life member of ISTE & Institutional Member of CSI.

Milind E Rane : received his BE degree in Electronics engineering from University of Pune and M Tech in Digital Electronics from Visvesvaraya Technological University, Belgaum, in 1999 and 2001 respectively. His research interest includes image processing, pattern recognition and Biometrics Recognition